Accepted Manuscript online: 2022-09-21 Article published online: 2022-12-15

Effect of adding acetic acid when performing magnifying endoscopy with narrow band imaging for diagnosis of Barrett's esophageal adenocarcinoma

OPEN ACCESS

Authors
Yohei Ikenoyama*,1,2, Kyosuke Tanaka*,1,2, Yuhei Umeda1,2, Yasuhiko Hamada1, Hiroki Yukimoto1, Reiko Yamada1, Junya Tsuboi1, Misaki Nakamura2, Masaki Katsurahara2, Noriyuki Horiki1, Hayato Nakagawa1,2

Institutions
1 Department of Gastroenterology and hepatology, Mie University Graduate School of Medicine, Tsu, Japan
2 Department of Endoscopy, Mie University Hospital, Tsu, Japan

submitted 19.5.2022
accepted after revision 20.9.2022
published online 22.9.2022

Bibliography
Endosc Int Open 2022; 10: E1528–E1536
DOI 10.1055/a-1948-2910
ISSN 2364-3722

Georg Thieme Verlag KG, Rüdigerstraße 14, 70469 Stuttgart, Germany

Corresponding author
Kyosuke Tanaka MD, PhD, Department of Endoscopy, Mie University Hospital, 2-174 Edobashi, Tsu, Mie, 514-8507, Japan
Fax: +81-59-231-5562
kyosuket@med.mie-u.ac.jp

ABSTRACT

Background and study aims Magnifying endoscopy with narrow band imaging (M-NBI) was developed to diagnose Barrett's esophageal adenocarcinoma (BEA); however, this method remains challenging for inexperienced endoscopists. We aimed to evaluate a modified M-NBI technique that included spraying acetic acid (M-AANBI).

Patients and methods Eight endoscopists retrospectively examined 456 endoscopic images obtained from 28 patients with 29 endoscopically resected BEA lesions using three validation schemes: Validation 1 (260 images), wherein the diagnostic performances of M-NBI and M-AANBI were compared – the dataset included 65 images each of BEA and non-neoplastic Barrett's esophagus (NNBE) obtained using each modality; validation 2 (112 images), wherein 56 pairs of M-NBI and M-AANBI images were prepared from the same BEA and NNBE lesions, and diagnoses derived using M-NBI alone were compared to those obtained using both M-NBI and M-AANBI; and validation 3 (84 images), wherein the ease of identifying the BEA demarcation line (DL) was scored via a visual analog scale in 28 patients using magnifying endoscopy with white-light imaging (M-WLI), M-NBI, and M-AANBI.

Results For validation 1, M-AANBI was superior to M-NBI in terms of sensitivity (90.8 % vs. 64.6 %), specificity (98.5 % vs. 76.9 %), and accuracy (94.6 % vs. 70.4 %) (all $P<0.05$). For validation 2, the accuracy of M-NBI alone was significantly improved when combined with M-AANBI (from 70.5 % to 89.3 %; $P<0.05$). For validation 3, M-AANBI had the highest mean score for ease of DL recognition (8.75) compared to M-WLI (3.63) and M-NBI (6.25) (all $P<0.001$).

Conclusions Using M-AANBI might improve the accuracy of BEA diagnosis.

Introduction

Barrett's esophagus (BE) is defined as columnar metaplasia of the distal esophagus. It involves abnormal cellular changes in the esophageal mucosa and is considered a precursor of BE

* These authors contributed equally to this article.

adenocarcinoma (BEA) [1], the incidence rate of which has been rapidly increasing in Western countries [2]. In Asian countries, including Japan, the incidence of BEA has also risen owing to an increase in the prevalence of obesity and gastroesophageal reflux disease as a consequence of lower *Helicobacter pylori* infection rates [3,4].

The prognosis of BEA is poor when the disease is diagnosed in an advanced stage [5] but is relatively favorable when treated while still in its superficial stage [6]. Therefore, its early detection is critically important; however, identifying superficial BEA is often difficult. In Western countries, the Seattle protocol for BE surveillance recommends that four-quadrant biopsy specimens be acquired at intervals of 1 to 2 cm [7]. However, random biopsies can lead to numerous sampling errors, and only 4 % to 5 % of BEs are discovered using this method [8–10]. Owing to such limitations, various endoscopic imaging techniques such as narrow band imaging (NBI), acetic acid chromoendoscopy (AAC), and endoscopy-based confocal laser endomicroscopy were developed to improve the diagnosis of superficial BEA [11]; among these, NBI has been the most widely researched.

To diagnose neoplastic lesions in patients with BE, several groups proposed classifications based on mucosal and vascular patterns visualized using magnifying endoscopy with NBI (M-NBI); however, these classifications did not markedly improve lesion detection owing to the complexity and diversification of vascular patterns [12–15]. To address these issues, the Japan Esophageal Society Barrett's esophagus (JES-BE) working group proposed a simpler M-NBI classification [16] that is based on representative early gastric cancer diagnostic criteria [17]. Although a study to validate this method showed promising diagnostic accuracy and interobserver agreement, it was conducted only by endoscopists at high-volume academic centers [18].

In contrast, a recent meta-analysis revealed that AAC was effective [19]. Acetic acid causes reversible acetylation of BE nucleoproteins and vascular congestion, which leads to highlighting microstructural patterns. However, there have been no dedicated studies on the usefulness of M-NBI that incorporates acetic acid spraying (M-AANBI). In addition, we are aware of no study that directly compared the diagnostic accuracy of M-AANBI with that of M-NBI. Hence, this study aimed to determine the ability of M-AANBI to detect BEA and compare it to that of M-NBI when used by either expert or non-expert endoscopists.

Patients and methods

Patients

This retrospective study included consecutive patients with BEA who underwent endoscopic submucosal dissection (ESD) between July 2005 and November 2021 at Mie University Hospital. Operable patients with a preoperative diagnosis of early-stage BEA were eligible for ESD. During the study period, 34 BEA lesions from 33 patients were evaluated with preoperative M-NBI/M-AANBI. Of these, four samples lacking images of either M-NBI or M-AANBI and one with low-quality endoscopic images were excluded; hence, 29 BEA lesions from 28 patients were retrospectively analyzed. The study was approved by the local ethics committee and was conducted according to the ethical standards laid out in the Declaration of Helsinki. The requirement for written informed consent was waived owing to the retrospective nature of the study. Instead, detailed information about the study was available to the public on our institutional website, and patients were offered the opportunity to opt out.

Definitions of BE, BEA, and non-neoplastic BE (NNBE)

BE was defined as an esophagus in which any portion of the normal distal squamous epithelial lining was replaced by metaplastic columnar epithelium as clearly visible endoscopically ≥ 1 cm above the esophagogastric junction and confirmed histopathologically [20]. The esophagogastric junction was defined as the end of the lower esophageal palisade vessels or upper limit of the gastric fold [21,22].

BEA was defined as adenocarcinoma that arose from BE as verified endoscopically and histologically, including non-invasive well-differentiated adenocarcinoma (high grade) that is equivalent to high-grade dysplasia in Western countries. NNBE was defined as the mucosa adjacent to the BEA that was resected during the ESD procedure.

Evaluation of endoscopic findings

All endoscopic images were obtained using a magnifying endoscope (GIF-Q240Z, GIF-H260Z, or GIF-H290Z; Olympus Corp., Tokyo, Japan) and an endoscopic system with NBI (EVIS LUCERA ELITE or EVIS LUCERA SPECTRUM; Olympus Corp.). A distal attachment (D-201-11804, D-201-11804, MAJ-1989, or MAJ-1990; Olympus Corp.) was placed on the tip of the endoscope to maintain a suitable focusing distance during magnification.

Tumor size, surface color, and macroscopic type were evaluated using white-light endoscopy. M-NBI was performed with optimal foci to evaluate mucosal and surface patterns according to the JES-BE classification [16]. Subsequently, 1.5 % acetic acid was sprayed onto the lesion with a 20-mL syringe at low pressure, and M-AANBI images were obtained and evaluated as detailed below. Non-magnifying NBI was performed before each M-NBI or M-AANBI session; alternating between magnified and non-magnified images helped identify the lesion section that was assessed.

Histopathological evaluation

All BEA lesions were resected using the ESD procedure. Each resected specimen was cut into 2 mm slices after formalin fixation; the histological type, size, depth of invasion, and margins (horizontal/vertical) were then evaluated. The pathological diagnosis was performed based on hematoxylin-eosin staining by two expert pathologists, who were blinded to endoscopic findings, according to the Japanese Classification of Esophageal Cancer [22]. The depth of tumor invasion was recorded as the T category; T1a and T1b were defined as tumors confined to the mucosa and submucosa, respectively. The extent of BEA was pathologically evaluated and compared to the endoscopic de-

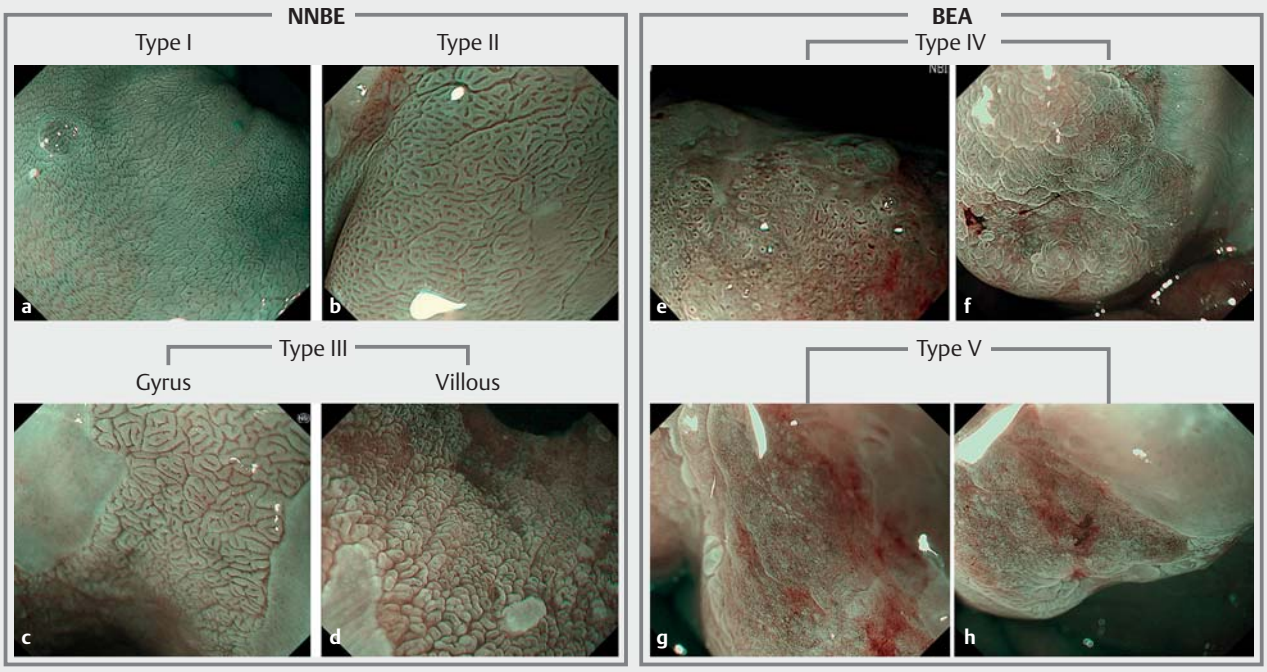

▶ **Fig. 1** Classifications of BEA/NNBE surface patterns using M-AANBI. The surface patterns of BEA and NNBE obtained using M-AANBI were classified into five types. **a** Small round pits of uniform size and shape (type I); **b** Slit-like pits (type II); **c** Gyrus pattern (type III); **d**, Villous pattern (type III); **e**, **f** Irregular arrangement and size (type IV); **g, h** Destructive pattern (type V); The characteristic surface patterns of NNBE were types I-III, while those of BEA were types IV and V. BEA, Barrett's esophageal adenocarcinoma; NNBE, non-neoplastic Barrett's esophagus; M-AANBI, magnifying endoscopy with narrow band imaging plus acetic acid spraying.

marcation line (DL), which was confirmed by comparison to the pathological BEA border.

Derivation study for developing BEA/NNBE classifications (phase 1)

In phase 1, two endoscopists (Y.I. and K.T.) evaluated 60 high-quality M-AANBI images of BEA and NNBE based on the AAC classification for gastric cancer [23]. Disagreements between the raters were resolved through discussion. The images were independent of those used for validation.

The characteristic surface patterns of BEA/NNBE were classified into five types as follows: type I, small round pits of uniform size and shape (▶ **Fig. 1a**); type II, slit-like pits (▶ **Fig. 1b**); type III, gyrus and villous patterns (▶ **Fig. 1c, d**); type IV, irregular arrangement and size (▶ **Fig. 1e**); and type V, destructive pattern (▶ **Fig. 1f**).

Validation studies (phase 2)

In phase 2, we conducted three validation studies to evaluate the diagnostic performance of M-AANBI. The images were examined by four expert endoscopists (Y.U., H.Y., Y.H., and M.K.) and four non-expert endoscopists (A.H., S.S., I.A., and W.Y.). We defined experts as operators who had experience with more than 100 M-NBI and M-AANBI procedures and non-experts as those who had experience with fewer than 20 such procedures. Non-expert endoscopists were provided a short explanation of M-AANBI-based diagnosis of BEA/NNBE (according to our developed classification) prior to their participation.

Validation 1 (main validation): Comparing the diagnostic performances of M-NBI and M-AANBI

An independent validation dataset was prepared to compare the accuracies of M-NBI and M-AANBI when diagnosing BEA. Based on the sample size (described below), the validation dataset included 130 each of M-NBI- and M-AANBI-acquired images; 65 BEA and 65 NNBE images were obtained with each of these two modalities. All images were randomized and verified, and each endoscopist then made a diagnosis of BEA or NNBE while assigning a confidence level (high/low) for each image. Agreement among the raters was quantified using Fleiss' kappa coefficient.

Validation 2: Changes in diagnostic performance owing to combining M-AANBI and M-NBI

To evaluate the effect of combining M-AANBI with M-NBI on diagnosis, 56 pairs of M-NBI and M-AANBI images acquired from the same lesion areas (28 BEA and 28 NNBE) were prepared. First, endoscopists performed their diagnoses using only M-NBI images. Subsequently, they re-diagnosed the samples using both M-NBI and M-AANBI; the difference in diagnostic performance between these two methods was then evaluated

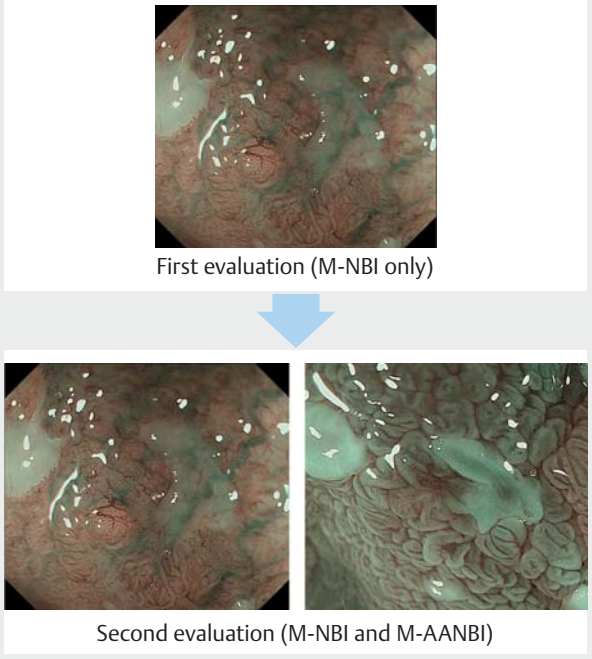

▶ **Fig. 2** Evaluating changes in diagnostic performance when using both M-AANBI and M-NBI. The first evaluation was performed using M-NBI only: a second evaluation was then performed using both M-NBI and M-AANBI. Abbreviations: M-AANBI, magnifying endoscopy with narrow band imaging plus acetic acid spraying; M-NBI, magnifying endoscopy with narrow band imaging.

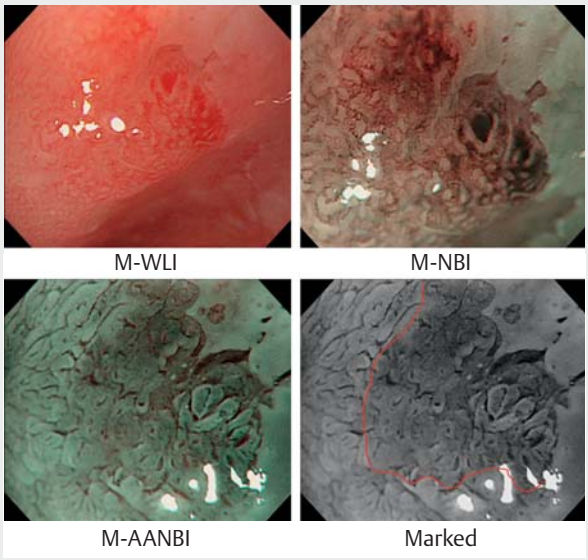

▶ **Fig. 3** Magnifying endoscopic images of the DL of BEA (same area). Abbreviations: DL, demarcation line; BEA, Barrett's esophageal adenocarcinoma; M-NBI, magnifying endoscopy with narrow band imaging; M-WLI, magnifying endoscopy with white-light imaging; M-AANBI, magnifying endoscopy with narrow band imaging plus acetic acid spraying; "Marked," marked image of the DL superimposed on the magnifying endoscopic image.

(▶ **Fig. 2**). Agreement among the raters was quantified using Fleiss' kappa coefficient.

Validation 3: Evaluating the ease of recognizing the DL using three methods

The DL was defined as the endoscopic border between the background non-cancerous and cancerous mucosae [24–26]; this has been confirmed to be consistent with pathological findings. DL recognition in the BEA samples of 28 patients was evaluated using three different methods: magnifying endoscopy with white-light imaging (M-WLI), M-NBI, and M-AANBI. For each lesion, three images of the same DL area were arranged on one slide for examination (▶ **Fig. 3**). Each endoscopist was instructed to score the ease of DL recognition when using each of these methods according to a visual analog scale (VAS), which was graded from 0 to 10 wherein 0 represented "invisible" and 10 represented "perfect visibility".

Sample size determination and statistical analysis

A pilot study was conducted to determine the appropriate sample size. Four expert endoscopists (Y.U., H.Y., Y.H., and M.K.) and four non-expert endoscopists (A.H., S.S., I.A., and W.Y.) evaluated 40 M-NBI and 40 M-AANBI images; 20 BEA and 20 NNBE images were examined using each modality. The mean diagnostic accuracies were 72.5 % for M-NBI and 85.6 % for M-AANBI. According to McNemar's test, 130 pairs of M-NBI and M-AANBI images were required to achieve a power of > 90 % (assuming a two-sided alpha of 0.05) based on eight diagnostic accuracy ratings from as many endoscopists.

Categorical variables are summarized as frequencies and percentages, while quantitative variables are presented as means and standard deviations. The performance of BEA diagnosis was determined by calculating the sensitivity, specificity, and accuracy for each endoscopist and the overall group. The interobserver agreement among endoscopists was calculated using Fleiss' kappa, with the strength of each agreement graded using the kappa value (< 0.20 = poor, 0.21–0.40 = fair, 0.41–0.60 = moderate, 0.61–0.80 = substantial, and 0.81–1.00 = almost perfect) [27]. Fisher's exact test was used to compare M-AANBI findings. The differences in the diagnostic test results between M-NBI and M-AANBI were analyzed using the McNemar's test. The average scores reflecting the ease of DL recognition using the three methods were compared using the Friedman test and Bonferroni's multiple comparison test. $P < 0.05$ was considered indicative of statistical significance in all tests. All calculations were performed using EZR version 1.27 (Saitama Medical Center, Jichi Medical University, Japan) [28].

▶ **Table 1** Clinicopathological characteristics of patients with BEA.

Patient characteristics (n = 28)	
Age, mean ± SD, years (range)	73.6 ± 9.6 (50–92)
Sex, male/female, n	24/4
Circumferential length of BE, mean cm (range)	2.2 ± 3.1 (0–15)
Maximal length of BE, mean cm (range)	3.4 ± 2.9 (1–15)
Lesion characteristics (n = 29)	
Size	
▪ Diameter, mean ± SD, mm (range)	20.5 ± 12.3 (6–53)
▪ <20 mm, n (%)	16 (55.2)
▪ ≥20 mm, n (%)	13 (44.8)
Macroscopic type, n (%)	
▪ Protruded (0-Is)	3 (10.3)
▪ Elevated (0-IIa)	7 (24.1)
▪ Flat (0-IIb)	4 (13.8)
▪ Depressed (0-IIc)	15 (51.7)
Color, n (%)	
▪ Whitish/isochromatic	10 (34.5)
▪ Reddish	19 (65.5)
Dominant histopathology, n (%)	
▪ Well-differentiated adenocarcinoma	25 (86.2)
▪ Moderately differentiated adenocarcinoma	3 (10.3)
▪ Poorly differentiated adenocarcinoma	1 (3.4)
Depth of invasion	
▪ T1a, n (%)	23 (79.3)
▪ T1b, n (%)	6 (20.7)

BEA, Barrett's esophageal adenocarcinoma; SD, standard deviation; BE, Barrett's esophagus; T1a, tumor confined to the mucosa; T1b, submucosal invasion.

Results

Patient characteristics

The clinical characteristics of patients with BEA and of their lesions are shown in ▶ **Table 1**. The mean patient age was 73.6 years (range, 50–92 years), and 79.2 % were men. Per the Prague criteria, the mean circumferential and maximal extents of BE were 2.2 cm and 3.4 cm, respectively. The mean tumor size was 20.5 mm; the most frequent macroscopic type was depressed (51.7 %), and 65.5 % of lesions had a reddish color. The dominant histopathology in most cases was well-differentiated adenocarcinoma (86.2 %), and tumor invasion in most cases was confined to the mucosa (79.3 %).

▶ **Table 2** Distribution of surface patterns in BEA and NNBE samples.

Surface patterns of M-AANBI	BEA	NNBE	*P* value[1]
Types I or II or III, n (type I/type II/type III)	1 (0/0/1)	30 (4/11/15)	<0.001
Type IV or V, n (type IV/type V)	29 (26/3)	0 (0/0)	

BEA, Barrett's esophageal adenocarcinoma; NNBE, non-neoplastic Barrett's esophagus.
[1] Fisher's exact test.

Derivation study (phase 1)

The assessment of surface patterns on BEA/NNBE using M-AANBI is shown in ▶ **Table 2**. The characteristic surface patterns of NNBE were wholly type I, type II, or type III. In contrast, almost all BEA images had two characteristic surface patterns (type IV or type V [$P<0.001$]). Therefore, type IV and V surface patterns observed on M-AANBI were deemed as predictive of BEA.

Validation studies (phase 2)

Validation 1 (main validation): Comparing the diagnostic performances of M-NBI and M-AANBI

▶ **Table 3** shows the diagnostic performance, interobserver agreement (κ value), and confidence levels for predicting BEA according to the validation 1 scheme. For M-NBI, the mean accuracy, sensitivity, and specificity among all endoscopists were 65.8 %, 61.7 %, and 69.8 %, respectively; in comparison, the values for M-AANBI were 91.1 %, 86.3 %, and 95.2 %, respectively. All parameters were significantly higher when using M-AANBI than with M-NBI among all eight endoscopists ($P<0.05$).

The accuracy of M-NBI was significantly higher in the expert group than in the non-expert group (70.0 % vs. 61.5 %, $P<0.05$). However, both groups achieved high accuracy with M-AANBI, with no difference between them.

The interobserver agreement among endoscopists was fair for M-NBI ($\kappa = 0.25$) and substantial for M-AANBI ($\kappa = 0.65$). Moreover, the proportion of high confidence for M-AANBI was greater than that for M-NBI (75.2 % vs. 53.3 %, $P<0.001$); both the expert and non-expert groups had similar tendencies.

Validation 2: Changes in diagnostic performance owing to combining M-AANBI and M-NBI

The results of validation 2-related analyses are presented in ▶ **Table 4**. The mean accuracy, sensitivity, and specificity of BEA diagnosis using M-NBI alone were 68.5 %, 64.6 %, and 73.2%, respectively. When using both M-NBI and M-AANBI, these values improved to 87.3 %, 85.7 %, and 90.6 %, respectively; the accuracy was significantly greater than that of M-NBI alone ($P<0.05$). The interobserver agreement when using M-NBI alone was fair ($\kappa = 0.31$), whereas that when combining M-NBI and M-AANBI was substantial ($\kappa = 0.69$). The high confi-

▶ **Table 3** Diagnostic performance of M-NBI and M-AANBI in terms of detecting BEA.

Raters	Modalities	Accuracy, % (95 % CI)	Sensitivity, % (95 % CI)	Specificity, % (95 % CI)	IO agreement *K* value (95 %CI)	High confidence rate, % (95 % CI)
All	M-NBI	65.8 (61.1–70.5)	61.7 (50.3–73.1)	69.8 (58.9–80.7)	0.25 (0.21–0.28)	53.3 (41.0–65.5)
	M-AANBI	91.1[1] (85.7–96.4)	86.3[1] (76.6–96.1)	95.2[1] (91.0–99.4)	0.65 (0.61–0.68)	75.2[1] (64.9–85.5)
Experts	M-NBI	70.0 (66.1–73.9)	64.6 (38.6–90.7)	75.4 (55.1–95.7)	0.38 (0.31–0.45)	61.2 (34.9–87.4)
	M-AANBI	91.3[1] (78.3–104.4)	85.0[1] (57.8–112.2)	97.7[1] (95.2–100.1 %)	0.64 (0.56–0.72)	81.7[1] (58.4–100.5)
Non-experts	M-NBI	61.5 (54.4–68.7)	58.5 (39.7–78.0)	64.2 (44.6–83.9)	0.33 (0.26–0.40)	45.4 (32.9–57.9)
	M-AANBI	90.8[1] (82.2–99.3)	87.7[2] (81.1–94.3)	92.7[1] (82.6–102.8)	0.66 (0.59–0.73)	68.7

BEA, Barrett's esophageal adenocarcinoma; M-NBI, magnifying narrow band imaging; M-AANBI, magnifying narrow band imaging plus acetic acid spraying; CI, confidence interval; IO, interobserver.
[1] $P<0.001$, vs. M-NBI using McNemar's test.
[2] $P<0.01$, vs. M-NBI using McNemar's test.

▶ **Table 4** Diagnostic performance parameters before/after adding M-AANBI to M-NBI.

Modalities	Accuracy mean, % (95 % CI)	Sensitivity mean, % (95 % CI)	Specificity mean, % (95 % CI)	IO agreement *K* value (95 %CI)	High confidence rate, % (95 % CI)
M-NBI	68.5 (62.9–74.2)	64.6 (56.2–73.2)	73.2 (61.3–85.2)	0.31 (0.26–0.36)	57.6 (45.0–70.2)
M-NBI + M-AANBI	87.3[1] (82.7–91.9)	85.7 (77.9–93.5)	90.6 (85.6–95.7)	0.69 (0.64–0.74)	76.3[2] (63.0–89.6)

M-NBI, magnifying endoscopy with narrow band imaging; M-AANBI, magnifying endoscopy with narrow band imaging plus acetic acid spraying; CI, confidence interval; IO, interobserver.
[1] $P<0.05$, vs. M-NBI using McNemar's test.
[2] $P<0.01$, vs. M-NBI using McNemar's test.

▶ **Table 5** Ease of demarcation line recognition when using M-WLI, M-NBI, and M-AANBI.

Modalities	All endoscopists	Experts	Non-experts
M-WLI, mean VAS ± SD	3.60 ± 1.27	3.53 ± 1.28	3.68 ± 1.41
M-NBI, mean VAS ± SD	6.16 ± 1.36[1]	6.16 ± 1.53[1]	6.16 ± 1.38[1]
M-AANBI, mean VAS ± SD	8.40 ± 0.76[12]	8.41 ± 0.82[12]	8.40 ± 0.92[12]

VAS, visual analog scale; M-WLI, magnifying endoscopy with white-light imaging; M-NBI, magnifying endoscopy with narrow band imaging; M-AANBI, magnifying endoscopy with narrow band imaging plus acetic acid spraying; SD, standard deviation.
[1] $P<0.001$, vs. M-WLI using Friedman's test.
[2] $P<0.001$, vs. M-NBI using Friedman's test.

dence rate improved from 57.6 % to 76.3 % when using both modalities.

Validation 3: Evaluating the ease of recognizing the DL using three methods

As shown in ▶ **Table 5**, the mean VAS scores for the ease of DL recognition as evaluated by all endoscopists were 3.60 ± 1.27 for M-WLI, 6.16 ± 1.36 for M-NBI, and 8.40 ± 0.76 for M-AANBI;

the differences between these scores (compared using the Friedman test) were significant ($P<0.001$). Using Bonferroni's multiple comparison test, the mean VAS score of M-AANBI was significantly higher than those of the other two methods, with M-NBI scoring significantly higher than M-WLI. Similar trends were observed in both the expert and non-expert groups ($P<0.001$).

Discussion

This study was the first to demonstrate the usefulness of M-AANBI in BEA diagnosis through direct comparison with M-NBI. The diagnostic accuracy, sensitivity, specificity, interobserver agreement, and confidence level of M-AANBI were significantly higher than those of M-NBI. Furthermore, combining M-NBI with M-AANBI produced an additive effect in terms of improving diagnostic accuracy; M-AANBI also tended to facilitate DL recognition.

To date, several NBI classifications for the diagnosis of BEA have been developed; however, they have proven to be complicated with limited diagnostic abilities [12–15], rendering them inadequate for use in clinical practice. In 2016, the Barrett's International NBI Group (BING) constructed a simpler NBI classification for differentiating between dysplasia and non-dysplasia and demonstrated high diagnostic performance for the former (overall accuracy: 85.4%, sensitivity: 80.4%, and specificity: 88.4%) and substantial interobserver agreement ($\kappa=0.681$) [29]. However, this validation was performed only by experts, and it remained unclear whether a similar diagnostic performance could be achieved by non-experts.

Subsequently, the JES-BE classification that was based on the typical M-NBI diagnostic criteria for early gastric cancer was proposed [16, 17]. BEA is diagnosed by an irregular mucosal or vascular pattern; the criteria were further modified to include the flat pattern originally regarded to be physiological. The JES-BE classification has been reported to have a high diagnostic ability (overall accuracy, 91%; sensitivity, 87%; and specificity, 97%) and high interobserver agreement ($\kappa=0.77$); however, that study was single-armed and could not be compared with other representative modalities such as M-AANBI [18]. Although the JES-BE classification was useful even for non-experts with little experience in diagnosing BEA, they were engaged in high-volume or academic centers and had substantial experience using magnification endoscopy for detecting early gastric cancer. Given that the JES-BE classification is based on the criteria used for detecting early gastric cancer, the existing familiarity of operators with magnification endoscopy may have affected the results; hence, the versatility of this classification in clinical practice remains unknown. With respect to this point, when we performed our tests on non-experts, the accuracy of M-NBI for BEA diagnosis using the JES-BE classification was significantly lower than it was among experts.

AAC has been reported to be a useful technique for BEA diagnosis [19]. Acetic acid changes the color of the BE epithelial surface to white, making it easier to recognize microstructural patterns. AAC is easy, safe, inexpensive, and effective, particularly for lesions with blood oozing on the surface; however, its superiority with respect to M-AANBI remains unknown as this question was not the focus of this study. Moreover, inflammatory changes can lead to incorrect BEA diagnoses when using AAC because of the rapid loss of acetowhitening [30]. Despite limited studies on the usefulness of M-AANBI in diagnosing BEA [31], it is better suited to avoid such misdiagnoses.

We previously classified surface patterns when using AAC in the stomach into five types, as described above [23]. When planning our current study, this classification was applied to differentiate BEAs from NNBEs (▶ **Fig. 1**); its use with M-AANBI showed a high diagnostic ability (overall accuracy, 91.1%; sensitivity, 86.3%; and specificity, 95.2%). All these parameters were superior to those of M-NBI. Although we provided a short tutorial for the diagnostic classification of M-AANBI to non-experts who had little experience with M-NBI and M-AANBI, the accuracy of BEA diagnosis by non-experts was high when using M-AANBI (equivalent to that of experts). Furthermore, the diagnostic performance and certainty were significantly improved by performing both M-AANBI and M-NBI. M-NBI-based diagnosis normally requires observation at high magnification to evaluate not only the structure but also the vascular pattern. However, since M-AANBI only examines structural patterns, it is possible to establish diagnoses with low magnification that emulates non-magnification; hence, this method is easy to use for endoscopists accustomed only to NBI in Western countries. Furthermore, M-AANBI may be utilized without magnification when using high-resolution endoscopes, which are likely to become more common in the future. Notably, the interobserver agreement was fair for M-NBI ($\kappa=0.25$) whereas the value for M-AANBI was substantial ($\kappa=0.65$). This indicates that M-NBI is subjective and difficult to interpret, while M-AANBI is an objective diagnostic method for all endoscopists including non-experts.

Identifying the DL between BEA and NNBE is generally considered difficult [32]. Since BE exhibits heterogeneous mucosal patterns of intestinal metaplasia, false DLs can be designated in NNBEs; this is also one of the reasons it is difficult to recognize the precise DL between BEA and NNBE. The ease of DL recognition using M-WLI was also low in the current study, whereas M-AANBI recognized the DL much more readily than M-NBI and M-WLI (▶ **Table 5**).

Artificial intelligence (AI) has recently allowed for remarkable progress in image recognition of gastrointestinal lesions [33]. A Previous study found that AI-based techniques are highly reliable for diagnosing gastric cancer using M-NBI [34]; furthermore, Ling et al. reported a unique AI system for identifying the DL in gastric cancer [35]. As such, AI may also be useful for the qualitative diagnosis of BEA and identification of the DL using M-AANBI.

This study had certain limitations. First, it was a retrospective study that used selected endoscopic images, and selection bias toward high-quality images existed. However, considering that physicians can observe all lesions in real-time in clinical practice, using high-quality images ought to be acceptable. Second, since this was a detailed comparative study of M-AANBI and M-NBI, validation was only performed on a cohort from our own institution. Third, the results were based on a small

sample size, and several images were extracted from the same lesion. Despite our best efforts to avoid it, some images may have been of overlapping sections of a given lesion. Hence, more data derived from a larger number of cases (including from multicenter prospective studies) are required to improve the diagnostic yield of such endoscopic findings. Fourth, the validation 3 scheme, which measured the confidence of recognizing the DL with each of three modalities, may have a subjective aspect. However, an endoscopic diagnosis is essentially a series of subjective evaluations; furthermore, the evaluators were blinded to the greatest extent possible during testing. As such, subjective bias ought to have been minimized. Fifth, M-AANBI is not a standard practice technique at present, with concerns that the essential system with magnifying endoscope for M-NBI is more expensive than the conventional endoscopy system. Furthermore, the M-AANBI technique may be complicated for endoscopists who are not familiar with the use of magnifying endoscopes. However, the NBI instruments have increased in popularity and acetic acid is not expensive due to its use as a threefold vinegar dilution. Moreover, similar to M-AANBI diagnosis, a high-resolution non-magnifying endoscope with a combination of AAC and NBI may be sufficient for diagnosis of BEA. Sixth, this study evaluated images of exposed BEA areas; however, certain BEA areas can sometimes be covered with normal squamous epithelium in patients treated with proton pump inhibitors. Therefore, the usefulness of M-AANBI for qualitative diagnosis and DL detection in areas covered with squamous epithelium is unknown.

Conclusions

In conclusion, we demonstrated the usefulness of M-AANBI in diagnosing BEA and its superiority to M-NBI. Although the diagnostic ability of M-NBI was low among non-experts, that of M-AANBI was high, with good interobserver agreement among all endoscopists and non-experts alike. The results of this study suggest that M-AANBI is useful for BEA diagnosis by endoscopists of all experience levels, including non-experts who have little experience with magnifying endoscopy. In clinical practice, the use of M-AANBI in addition to M-NBI might be beneficial for BEA detection during surveillance endoscopy for BE and for DL recognition during ESD for BEA.

Competing interests

The authors declare that they have no conflict of interest.

References

[1] Desai TK, Krishnan K, Samala N et al. The incidence of oesophageal adenocarcinoma in non-dysplastic Barrett's oesophagus: a meta-analysis. Gut 2012; 61: 970–976

[2] Pohl H, Sirovich B, Welch HG. Esophageal adenocarcinoma incidence: are we reaching the peak? Cancer Epidemiol Biomarkers Prev 2010; 19: 1468–1470

[3] Hongo M, Nagasaki Y, Shoji T. Epidemiology of esophageal cancer: orient to occident. Effects of chronology, geography and ethnicity. J Gastroenterol Hepatol 2009; 24: 729–735

[4] Wang Z, Shaheen NJ, Whiteman DC et al. Helicobacter pylori infection is associated with reduced risk of Barrett's esophagus: an analysis of the Barrett's and esophageal adenocarcinoma consortium. Am J Gastroenterol 2018; 113: 1148–1155

[5] Mansour NM, Groth SS, Anandasabapathy S. Esophageal adenocarcinoma: screening, surveillance, and management. Annu Rev Med 2017; 68: 213–227

[6] Abe S, Ishihara R, Takahashi H et al. Long-term outcomes of endoscopic resection and metachronous cancer after endoscopic resection for adenocarcinoma of the esophagogastric junction in Japan. Gastrointest Endosc 2019; 89: 1120–1128

[7] Wang KK, Sampliner RE. Practice Parameters Committee of the American College of Gastroenterology. Updated guidelines 2008 for the diagnosis, surveillance and therapy of Barrett's esophagus. Am J Gastroenterol 2008; 103: 788–797

[8] Sharma P, McQuaid K, Dent J et al. A critical review of the diagnosis and management of Barrett's esophagus: the AGA Chicago Workshop. Gastroenterology 2004; 127: 310–330

[9] Falk GW, Ours TM, Richter JE. Practice patterns for surveillance of Barrett's esophagus in the United States. Gastrointest Endosc 2000; 52: 197–203

[10] Das D, Ishaq S, Harrison R et al. Management of Barrett's esophagus in the UK: overtreated and underbiopsied but improved by the introduction of a national randomized trial. Am J Gastroenterol 2008; 103: 1079–1089

[11] Thosani N, Abu Dayyeh BK. ASGE Technology Committee. et al. ASGE Technology Committee systematic review and meta- analysis assessing the ASGE Preservation and Incorporation of Valuable Endoscopic Innovations thresholds for adopting real- time imaging-assisted endoscopic targeted biopsy during endoscopic surveillance of Barrett's esophagus. Gastrointest Endosc 2016; 83: 684–698

[12] Singh M, Bansal A, Curvers WL et al. Observer agreement in the assessment of narrowband imaging system surface patterns in Barrett's esophagus: a multicenter study. Endoscopy 2011; 43: 745–751

[13] Silva FB, Dinis-Ribeiro M, Vieth M et al. Endoscopic assessment and grading of Barrett's esophagus using magnification endoscopy and narrow-band imaging: accuracy and interobserver agreement of different classification systems (with videos). Gastrointest Endosc 2011; 73: 7–14

[14] Curvers WL, Bohmer CJ, Mallant-Hent RC et al. Mucosal morphology in Barrett's esophagus: interobserver agreement and role of narrow band imaging. Endoscopy 2008; 40: 799–805

[15] Baldaque-Silva F, Marques M, Lunet N et al. Endoscopic assessment and grading of Barrett's esophagus using magnification endoscopy and narrow band imaging: impact of structured learning and experience on the accuracy of the Amsterdam classification system. Scand J Gastroenterol 2013; 48: 160–167

[16] Goda K, Fujisaki J, Ishihara R et al. Newly developed magnifying endoscopic classification of the Japan Esophageal Society to identify superficial Barrett's esophagus-related neoplasms. Esophagus 2018; 15: 153–159

[17] Muto M, Yao K, Kaise M et al. Magnifying endoscopy simple diagnostic algorithm for early gastric cancer (MESDA-G). Dig Endosc 2016; 28: 379–393

[18] Goda K, Takeuchi M, Ishihara R et al. Diagnostic utility of a novel magnifying endoscopic classification system for superficial Barrett's esophagus-related neoplasms: a nationwide multicenter study. Esophagus 2021; 18: 713–723

[19] Coletta M, Sami SS, Nachiappan A et al. Acetic acid chromoendoscopy for the diagnosis of early neoplasia and specialized intestinal meta-

plasia in Barrett's esophagus: a meta-analysis. Gastrointest Endosc 2016; 83: 57–67

[20] Fitzgerald RC, di Pietro M, Ragunath K et al. British Society of Gastroenterology guidelines on the diagnosis and management of Barrett's oesophagus. Gut 2014; 63: 7–42

[21] Emura F, Chandrasekar VT, Hassan C et al. Rio de Janeiro global consensus on landmarks, definitions, and classifications in Barrett's esophagus: World Endoscopy Organization Delphi Study. Gastroenterology 2022; 163: 84–96

[22] Japan Esophageal Society. Japanese classification of esophageal cancer, 11th Edition: part II and III. Esophagus 2017; 14: 37–65

[23] Tanaka K, Toyoda H, Kadowaki S et al. Features of early gastric cancer and gastric adenoma by enhanced-magnification endoscopy. J Gastroenterol 2006; 41: 332–338

[24] Yao K, Iwashita A, Tanabe H et al. Novel zoom endoscopy technique for diagnosis of small flat gastric cancer: a prospective, blind study. Clin Gastroenterol Hepatol 2007; 5: 869–878

[25] Yao K, Iwashita A, Kikuchi Y et al. Novel zoom endoscopy technique for visualizing the microvascular architecture in gastric mucosa. Clin Gastroenterol Hepatol 2005; 3: S23–S26

[26] Yao K, Anagnostopoulos GK, Ragunath K. Magnifying endoscopy for diagnosing and delineating early gastric cancer. Endoscopy 2009; 41: 462–467

[27] Landis JR, Koch GG. The measurement of observer agreement for categorical data. Biometrics 1977; 33: 159–174

[28] Kanada Y. Investigation of the freely available easy-to-use software "EZR" for medical statistics. Bone Marrow Transplant 2013; 48: 452–458

[29] Sharma P, Bergman J, Goda K et al. Development and validation of a classification system to identify high-grade dysplasia and esophageal adenocarcinoma in Barrett's esophagus using narrow-band imaging. Gastroenterology 2016; 150: 591–598

[30] Lambert R, Rey JF, Sankaranarayanan R. Magnification and chromoscopy with the acetic acid test. Endoscopy 2003; 35: 437–445

[31] Tanaka K, Toyoda H, Jaramillo E. Magnifying endoscopy in combination with narrow-band imaging and acetic acid instillation in the diagnosis of Barrett's esophagus.Niwa H, Tajiri H, Nakajima M, Yasuda K. New challenges in gastrointestinal endoscopy. Tokyo: Springer; 2008: 153–160

[32] Iwagami H, Kanesaka T, Ishihara R et al. Features of esophageal adenocarcinoma in magnifying narrow-band imaging. Dig Dis 2021; 39: 89–95

[33] Lui TKL, Tsui VWM, Leung WK. Accuracy of artificial intelligence-assisted detection of upper GI lesions: a systematic review and meta-analysis. Gastrointest Endosc 2020; 92: 821–830

[34] Ueyama H, Kato Y, Akazawa Y et al. Application of artificial intelligence using a convolutional neural network for diagnosis of early gastric cancer based on magnifying endoscopy with narrow-band imaging. J Gastroenterol Hepatol 2021; 36: 482–489

[35] Ling T, Wu L, Fu Y et al. A deep learning-based system for identifying differentiation status and delineating the margins of early gastric cancer in magnifying narrow-band imaging endoscopy. Endoscopy 2021; 53: 469–477